Evaluation of a MEMS based theft detection circuit for RFID labels

Damith C. Ranasinghe[*a], Peter H. Cole [a]
[a]School of Electrical & Electronic Engineering, Univ. of Adelaide, SA, Australia 5005

ABSTRACT

In the proliferation of RFID technology anti-theft labels are continuing to evolve. In the functional hierarchy of RFID labels the battery-powered labels are a set of higher class labels referred to as active labels. Often these labels are employed for the tagging of expensive goods, with aim of both tracking and preventing the theft of the item. The battery powering such active labels must have very low internal and external current drain in order to prolong the life of the battery while being in a state of functionality to signal a theft of the labelled item. However due to circuit complexity or the desired operating range the electronics may drain the battery more rapidly than desired and the label may not last the shelf life of the product.

The theft detection mechanism presented in this paper conserves power and thus prolongs the battery life of an active anti-theft label. A solution available for the development of such a theft detection circuit uses electroacoustic energy conversion using a MEMS device on a label IC to provide a high sensitivity result. This paper presents the results of an analysis conducted to evaluate the performance and the capabilities of such a theft detection circuit.

Keywords: MEMS, RFID, active labels, turn-on

1. INTRODUCTION

A simple illustration of the concept of a Radio Frequency Identification (RFID) system is provided in Figure 1. Here a transmitter of interrogation signals which is contained within an interrogator communicates via electromagnetic waves with an electronically coded label to elicit from the label a reply signal containing useful data characteristic of the object to which the label is attached. The reply signal is detected by a receiver in the interrogator and made available to a control system.

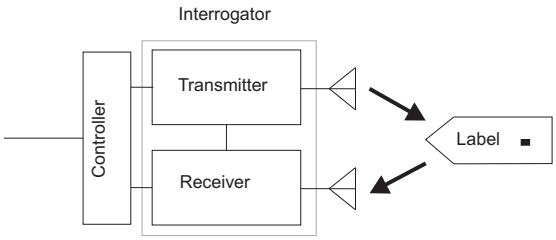

Figure 1: Illustration of an RFID system.

There is a wide range of operating principles for such a system [1,2]. The operating principle and operating frequency are driven principally by the application of the labelling system and the constraints provided by electromagnetic compatibility regulations, environmental noise, and the ability of fields to permeate a scanned region of space or to penetrate intervening materials. Applications are found in reliable and secure data collection, object or personal identification, authentication, anti-counterfeiting, theft detection and the detection of location of the scanned objects.

In a primary category of passive systems the most common operating principle is that of RF backscatter [1] in which a powering signal or communication carrier supplies power or command signals via an HF or UHF link. However the circuits within the label operate at RF or lower, and reply via sidebands generated by modulation, within the label, or part of the powering carrier. This approach combines the benefits of relatively good propagation of signals at HF and UHF and the low power of operation of microcircuits at RF or lower. Powering at UHF is employed when a longer

[*] damith@eleceng.adelaide.edu.au; phone (08) 8303 4119.

interrogation range (several meters) is required, and HF powering is employed when electromagnetic fields, which exhibit good material penetration and sharp spatial field confinement, are required or sometimes when a very low cost RFID system implementation is desired.

In the category of active labels the most common objective is to obtain a long range in a battery-assisted backscatter label. However other types of active labels may not use backscatter but instead use a battery for powering and transmitting requirements. This paper examines and presents a practicable solution for theft detection of high value tagged items by the implementation of a “screaming corridor”. The solution presented is capable of conserving battery power and thus extending the lifetime of the battery while providing a high level of security in theft detection by use of high performance long lifetime theft detection labels.

2. THEFT DETECTION CIRCUIT

The primary focus of this paper is on active labels that will be equipped with a power source (such as a paper battery). The interrogation of active labels requires the development of a mechanism for turning on the labels, as power conservation is an important factor that requires the labels to be turned off when not being interrogated, thus minimizing power loss to be only that caused by leakage currents within a battery. Creating a solution to turn-on an active label when the theft of a labelled item is taking place is a solution that suffices to address both theft detection and the need for power conservation of an active theft detection label.

Some active labels are expected to backscatter a reply with the logic circuits of the labels being powered from the onboard battery while other active labels are likely to be independent reply generating labels. An active backscattering label will modulate the powering carrier or a subcarrier to establish a communication link with the reader while using the battery to power the logic circuits of the label. However an active label that uses an independent source of power for generating a reply to a reader uses the onboard battery to power the transmitter of the label. This distinction is more apparent in the range of operation of the label. A reply from a backscattering label is very weak, and under RFID system operating under the US regulations for the ISM (Industrial, Scientific and Medical) band of 902-926 MHz (allowed transmit power in this band is 4W EIRP), a backscattered reply can be correctly decoded in the range of several tens of meters. However an active label with an independent source of power for reply generation will work in the range of several hundred meters.

There are number of practical options for a theft detection circuit for a battery powered RFID label. Although very low quiescent power theft detection circuits are possible, the requirement of increasing the lifetime of RFID labels (perhaps due to longer shelf life of the labelled product) demands a zero quiescent power theft detection circuit. The proposed theft detection circuit is a zero power turn-on circuit for active RFID labels that will rely on generating a voltage of the order of 1V that can turn a CMOS transistor from fully off to fully on when triggered by a low frequency large volume magnetic field.

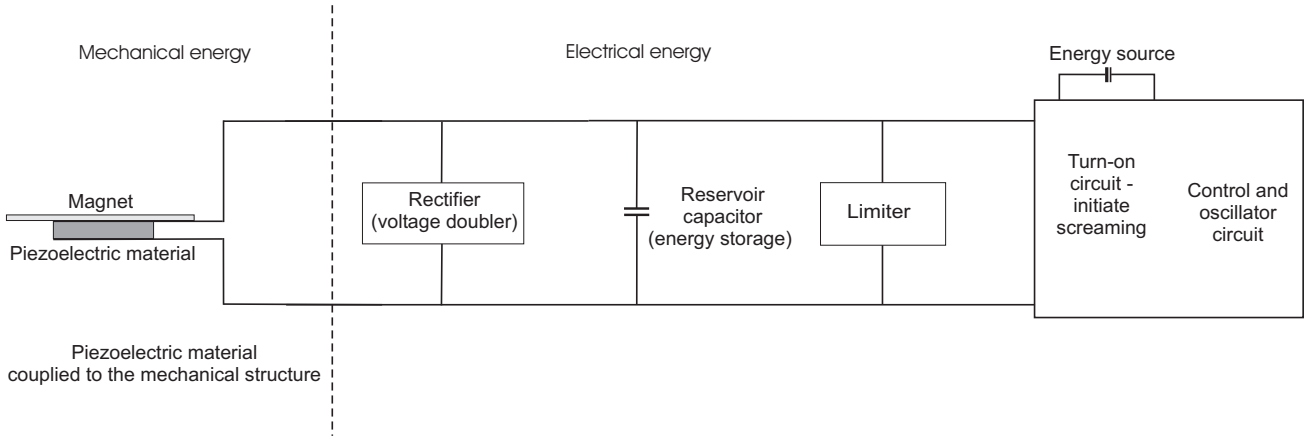

Figure 2: Components of the theft detection system.

The proposed approach utilizes a piezoelectric material to convert mechanical energy provided by an oscillating magnet into electric power as shown in Figure 2. There are four essential components described in Figure 2. The piezoelectric material coupled to a magnet (mechanical structure) is used to covert mechanical stress placed in the slab of piezoelectric material due to the forced oscillations induced on the magnet from an oscillating magnetic field, to electric power. The oscillating voltage is then rectified to provide a reliable 1 V to turn on the switch operated by a FET (refer to Figure 10 for turn-on circuit schematic) to a theft alert circuit which will cause the label to "scream" by alerting interrogators of the theft and also provide a beacon for tracking the item. The theft detection process is illustrated in Figure 3. The low frequency large volume magnetic field provides the trigger for the MEMS circuit. Such a field can be setup in and around the vicinity of a large corridor exit to turn the MEMS theft circuitry "on" when a thief attempts to flee with stolen goods.

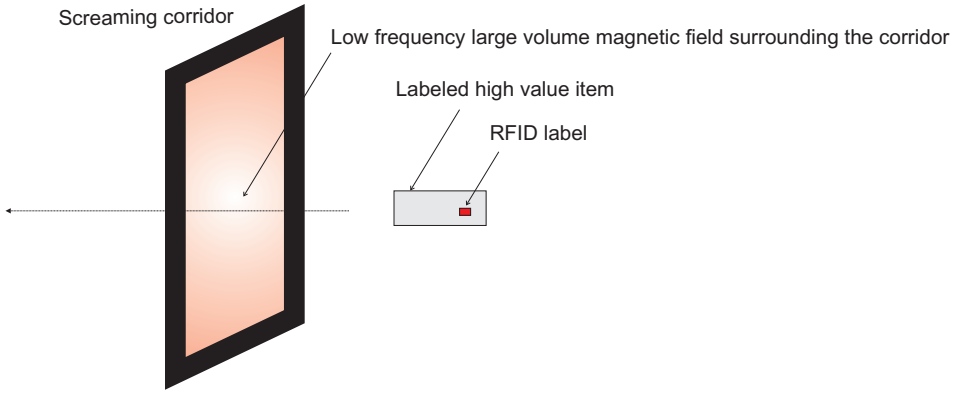

Figure 3: The "screaming corridor".

2.1. Magnetic-electoacoustic energy conversion system

A piezoelectric material acts as a transformer element between mechanical energy and electrical energy. When an external mechanical force applied to a piezoelectric material strains the element, the unit cells of the crystal shift and realign. This results in the development of an electrostatic potential between certain opposing faces of the element. The relationship between the applied force and the resulting electric charge is dependent upon a number of characteristics inherent to the material as well as its size, shape and mechanical distortion.

The concept outlined here depends on being able to generate a large volume low frequency magnetic field in the vicinity of the active labels to harness the required mechanical energy such that the oscillating magnetic field will influence the magnet to oscillate with sufficient energy to generate through the piezoelectric effect a voltage *V* that is adequate to turn on a FET.

The intended frequency of operation of the turn-on circuit should allow the creation of a large volume magnetic field without exceeding the electromagnetic regulations regarding radiation (field confinement without undue radiation). In addition the intended frequency of operation should not consume excessive power to create large volume interrogation fields, and the field created should not be easily screened. It is also important that the frequency be high enough such that ambient electromagnetic fields do not cause the turn on circuit to become operational unintentionally. All these considerations point to the use of a frequency around the LF electromagnetic spectrum. FCC electromagnetic compatibility regulations part 15, section 15.209 [4] has defined the use of the LF electromagnetic spectrum for general use while CEPT/ETSI has an unlicensed band from 119-135 kHz, among other bands in the LF spectrum. Considering that the frequency range less than 135 kHz is unlicensed and is available for general use around the world and taking note of the aforementioned considerations, 130 kHz was considered for creating a large volume, low frequency, magnetic field to power the turn-on circuit. It will be important to consider later the practically achievable magnetic field levels and any regulatory limits on them.

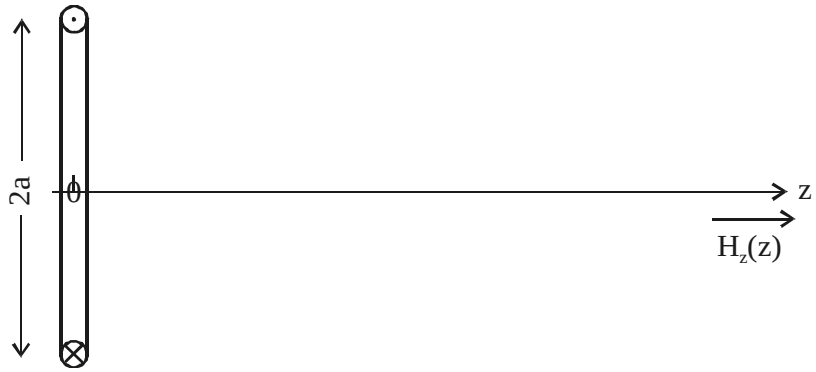

Figure 4: Geometry of the large coil

Consider, as shown in Figure 4, a single turn circular planar coil of diameter *d*, used to create at a distance *z* a magnetic field $H_z(z)$, at a frequency *f* when there is r.m.s current *I* flowing through the coil. Then the magnetic field at a distance *z* is given by equation 1. Figure 5 shows the variation of the magnetic field strength as a function of the normalized distance from the coil. Clearly, creating a large volume magnetic field requires the use of a large loop structure. The following analysis will consider such a structure.

$$H_z(z) = \frac{Ia^2}{2\left(a^2 + z^2\right)^{3/2}} \tag{1}$$

For the geometry considered in Figure 4, the total reactive power flowing per unit volume at a point where the magnetic field described by a real r.m.s. phasor **H** is given by

$$W_H = \omega\mu_0 |\mathrm{H}|^2 . \tag{2}$$

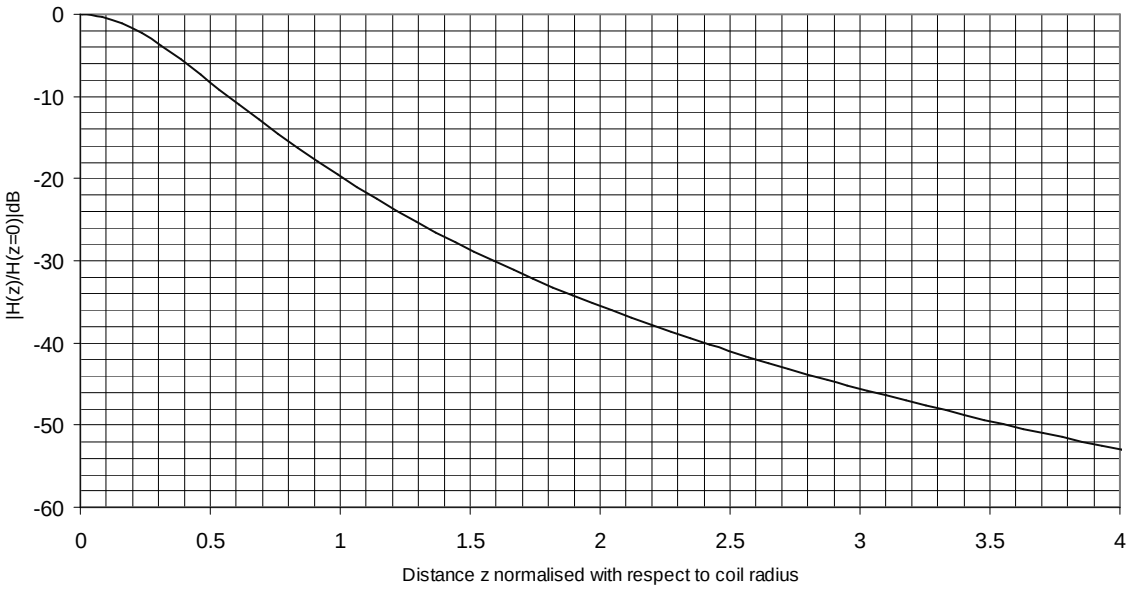

Figure 5: Relative magnetic field strength at a normalised distance (z/a) from a circular coil

In the situation where skin currents flow on surface of the coil conductor the self-inductance is given by

$$L = \frac{\mu_0 D}{2}\left[\log_e\left(\frac{8D}{d}\right) - 2\right]. \tag{3}$$

The power P dissipated by a r.m.s current I flowing in the coil is given by

$$P = I^2 R \tag{4}$$

where R is the resistance of the coil or is an effective resistance that lakes into account all losses in the resonant circuit formed by the coil and a tuning capacitor normally placed in parallel with a lossless capacitor.

The quality factor of resonance can be obtained using the resistance of the coil wire. At a frequency of 130 kHz the skin depth effects must be taken into consideration. The skin depth of copper at 130 kHz is 183 μm. Considering a practicable geometry for the coil the following parameters outlined in Table 1 can be used to evaluate the reactive power density at distance z from the centre of the coil (refer to Figure 4).

Description	**Symbol**	**Value**
Coil diameter	*D(2a)*	3 m
Diameter of the coil wire	*d*	10 mm
Power supplied	*P*	50 W
Frequency of operation	*f*	130 kHz

Table 1: Field generating coil configuration

A coil constructed with the dimensions outlined in Table 1 will have an inductance of L = 10.9011 μH while the effective quality factor of the coil is expected to be around 60 (however the calculated quality using the resistance of the coil based on its skin depth is a much higher value but in a practical implementation there are additional losses from tuning capacitors). The evaluations based on the following sections of the paper will assume a magnetic field strength created by a pair of coils with 50 W of power to supplied to each coil.

3. ANALYSIS

Electroacoustic energy conversion systems have traditionally been modelled using mass-spring damper systems [6 and 7]. However we have used coupling relations to analyse the feasibility of the proposal.

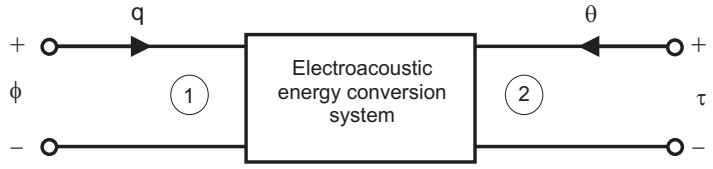

Figure 6: Representation of an electroacoutic conversion system [7].

2.2. Electroacoustic energy conversion

The energy conversion system outlined in Figure 6 can be formulated using a pair of electrical terminals and a pair of mechanical terminals as indicated in Figure 6. The quantities represented by ϕ and q are the instantaneous applied voltage and charge that has entered the electrical port, and τ and θ are the instantaneous applied torque and angular displacement at the mechanical port. The electromechanical system can thus be described by the following relationship [8].

$$\begin{bmatrix} q \\ \theta \end{bmatrix} = \begin{bmatrix} C_{11P} & C_{12P} \\ C_{21P} & C_{22P} \end{bmatrix} \begin{bmatrix} \phi \\ \tau \end{bmatrix} \tag{5}$$

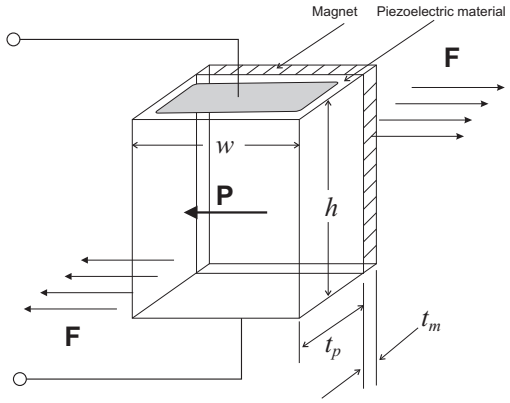

Figure 7: Magnet coupled to the piezoelectric material. Here **F** is the shearing force applied by the magnet and **P** is the direction of polarization of the piezoelectric material

In the above matrix, C_{11P} is the input capacitance at the electrical port with zero torque applied to the mechanical port. C_{11P} for the slab piezoelectric material can be calculated in the thin parallel plate approximation by

$$C_{11P} = \frac{\varepsilon^T \varepsilon_0 \, wh}{t_p} \tag{6}$$

Here ε^T is the relative dielectric constant under constant stress, t_p is the thickness of the piezoelectric material while l and w are the length and the width of the electrode plates respectively (refer to Figure 7). C_{22P} is the compliance of the piezoelectric structure given that the piezoelectric material compliance is s_P^E .

$$C_{22P} = \frac{s_P^E}{hwt_p}. \tag{7}$$

The off diagonal element C_{21P} is the angular displacement at port 2 when a voltage is applied to port 1 and no torque is applied to port 2. C_{12P} gives the charge entering port 1 when it is short circuit and a torque is applied to port 2.

2.3. Electrical power

A FET will require a turn on voltage of 1 V across the gate to turn it from an “off” state to an “on” state. This voltage is provided by the rectifying structure. Hence the voltage generated at the electrical port of the electroacoustic converter will have to serve an electrical load of approximately 1 pF and a series resistance of around 10 Ω presented by a Schottky diode. At the operational frequency range of 902-228 MHz, under FCC regulations, the electrical load is primarily the junction capacitance of the Schottky diode. Figure 8 shows the electroacoustic energy conversion system considering its electrical load.

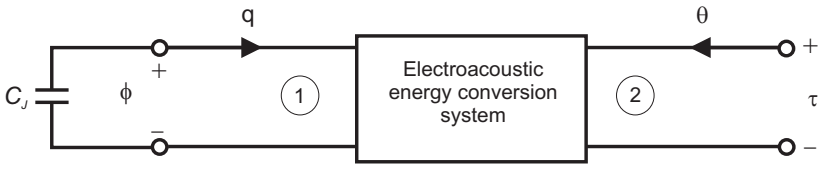

Figure 8: Representation of the electroacoutic energy conversion system with an electrical load.

The electroacoustic converter characterised above, connected to an external load of C_j will have a charge q developed at the port 1 when a torque τ is applied to port 2. The charge q is given by

$$q = -C_{11P}\phi \,. \tag{8}$$

Solving the matrix for ϕ gives

$$\phi = -\frac{C_{12P}\tau_P}{C_{11P} + C_J} \,. \tag{9}$$

Considering the dimensionless ration $r = C_J/C_{11}$

$$\phi = -\frac{C_{12P}\tau_P}{C_{11P}(1+r)} \tag{10}$$

Solving the matrix for equation 5 gives

$$\theta = -\frac{C_{12P}C_{21P}\tau_P}{C_{11P}(1+r)} + C_{22}\tau_P \tag{11}$$

We can define k^2 as [9]

$$k^2 = \frac{C_{12P}C_{21P}}{C_{11P}C_{22P}} \,. \tag{13}$$

For a piezoelectric material k^2 is described as the electromechanical coupling factor of the material. For a piezoelectric material the coupling factor can be simply described as

$$k^2 = \frac{\text{Mechanical energy converted to stored electrical energy}}{\text{Mechanical energy input}} \tag{12}$$

However for a structure in which we have uniform stress, strain, electric field and polarization it can be proved that the electromechanical coupling factor for the material is identical to that of the piezoelectric structure. Hence

$$\theta = \left[1 - \frac{k^2}{1+r}\right] C_{22P}\tau_P \,. \tag{14}$$

Thus we have an effective compliance for the capacitive loaded electroacoustic converter given by

$$C_{22eff} = \left[1 - \frac{k^2}{1+r}\right] C_{22P} \tag{15}$$

where C_{22P} is the open circuit compliance at the electrical port. Observing that θ is proportional to τ, the stored energy for a final torque τ applied to the mechanical port is given as

$$E_{MP} = \frac{1}{2}\left(1 - \frac{k^2}{1+r}\right) C_{22P}\tau^2 \,. \tag{16}$$

The energy E_M expended at the mechanical port will appear as stored energy in the capacitor C_J, hence the electrical energy E_E at the electrical port is given as

$$E_{EP} = \frac{1}{2} C_J \left(\frac{C_{12P}^2}{C_{11P}^2 (1+r)^2} \right) \tau^2 . \tag{17}$$

Using equations 16 and 17

$$\frac{E_{EP}}{E_{MP}} = \frac{rk^2}{(1+r)^2 - k^2(1+r)} . \tag{18}$$

Equation 18 gives the effective electromechanical coupling factor k_{eff}^2 for the piezoelectric structure as

$$k_{eff}^2 = \frac{rk^2}{(1+r)^2 - k^2(1+r)} . \tag{19}$$

2.4. Mechanical power

In a practical realisation of the turn-on circuit the mechanical stress on the structure is provided by the torque exerted on structure in Figure 7 by the oscillatory magnetic field. If the magnitude of the total toque on the composite structure is represented by the r.m.s phasor T_S and is provided by the torque exerted by the field on the magnet, then

$$T_S = \mu_0 v M H . \tag{20}$$

Where ρ is the material density, v is the volume of the magnet and M is the remnant magnetisation. It should be noted that equation 14 assumes that the direction of the magnetisation M is orthogonal to the magnetic field H.

The mechanical stress on the structure is provided by a permanent magnet excited by an oscillating magnetic field where the resulting energy E_{MS} of the structure flowing into the stiffness of the structure can be evaluated as

$$E_{MS} = \left| T_S \right|^2 C_{22S} . \tag{21}$$

C_{22S} is the total compliance of the structure at the mechanical port. C_{22S} is calculated as the harmonic mean of the effective compliance of the piezoelectric material C_{22eff} and the compliance C_{22M} of the magnetic structure. Thus, C_{22S} can be calculated as

$$C_{22S} = \frac{1}{\left(\frac{1}{C_{22M}} + \frac{1}{C_{22eff}} \right)} \tag{22}$$

where

$$C_{22M} = \frac{s_M^E}{hwt_m} \tag{23}$$

and s_M^E is the compliance of the magnetic material.

From the total mechanical stress placed on the structure, only the mechanical stress on the piezoelectric material will result in transferring electrical energy E_{MP} into the stiffness of the piezoelectric. That electrical energy is given as

$$E_{MP} = \frac{1}{2}\left|\mathrm{T_P}\right|^2 C_{22eff} \text{ where } \mathrm{T_P} = \mathrm{T_S}\left(\frac{C_{22S}}{C_{22eff}}\right). \tag{24}$$

2.5. Mechanical resonance

The section above evaluated the energy power flow into the stiffness of the piezoelectric material. It can be viewed that the piezoelectric material is placed under a shearing stress as the magnet inclines to oscillate at the frequency of the surrounding magnetic field. However, at the mechanical resonance frequency of the combined structure with a mechanical quality factor Q_m the voltage developed at the electrical port is multiplied by the quality factor of mechanical resonance Q_m. Thus the voltage at the electrical port is increased by a factor of Q_m. Hence the energy E_{EPR} stored in C_J at the electrical port is given by equation 24.

$$E_{EPR} = k_{eff}^2 Q_m^2 E_{MP} \tag{25}$$

Using equation 24,

$$E_{EPR} = \frac{1}{2} k_{eff}^2 \; Q_m^2 \omega \left|\mathrm{T_P}\right|^2 C_{22eff} \tag{26}$$

Hence a magnet with a volume v, and a magnetisation constant M will provide the following energy flow into the capacitor C_J at the electrical port.

$$E_{ERP} = \frac{1}{2} k_{eff}^2 Q_m^2 (Mv\mu_0)^2 \left|\mathrm{H}\right|^2 C_{22S}^2 \frac{1}{C_{22eff}} \tag{27}$$

2.6. Zero power turn-on requirements

The r.m.s voltage V_{EPR} can be calculated as follows

$$V_{EPR} = \sqrt{\frac{E_{ERP}}{C_J}} \tag{28}$$

For the production of a rectified output even to an open circuit load, a rectifying diode must experience across the junction capacitance a voltage of the order of or greater than the rectified output. Thus, the r.m.s voltage V_{TO} (V_{EPR}) available to turn on a FET can be calculated as follows

$$V_{TO} = \sqrt{k_{eff}^2 Q_m^2 (Mv\mu_0)^2 \left|\mathrm{H}\right|^2 C_{22S}^2 \frac{1}{C_J C_{22eff}}} \text{ where } k_{eff}^2 = \frac{rk^2}{(1+r)^2 - k^2(1+r)} \text{ and } C_{22eff} = \left[1 - \frac{k^2}{1+r}\right] C_{22P}. \tag{29}$$

In order for the theft detection circuit to activate V_{TO} must be about 1 V.

It should be noted here that in the event that the Schottky barrier diode junction capacitance is comparable to C_{11P}

$$k_{eff}^2 = \frac{k^2}{4 - 2k^2}. \tag{30}$$

4. PRACTICAL EVALUATION

Figure 9 outlines a possible schematic for a turn on circuit based on a piezoelectric source. It should be noted here that the power lost in the rectification process will not be considered here, however it is sufficient to say the turn-on voltage calculated is an absolute minimum turn on requirement. Nevertheless several circuits simulated showed that a voltage doubling rectifier used in the turn-on circuit is the optimal design that minimizes the diode losses.

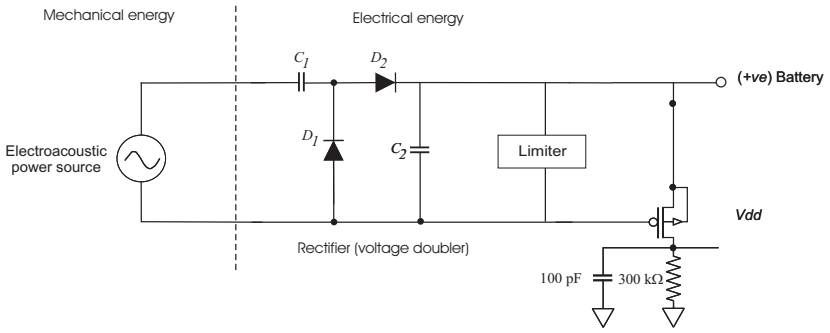

Figure 9: MEMS based theft detection turn on circuit schematic

The piezoelectric material chosen for practical evaluation purposes is PZT, largely due to its higher coupling coefficient. It can be seen from equation 20 that a large k^2 is a desired characteristic. There is a variety of different PZT ceramics available with a diversity of characteristics while some ceramics can be custom made with desired characteristics [10, 11]. However for the evaluation of the theft detection circuit a shear coupling coefficient, k_{15} of 0.69 and a frequency constant N_{15} of 1000 Hzm is used. Figure 10 shows the variation of the resonant frequency for a piezoelectric under a shearing stress. In order to ensure the efficient transfer of the energy density in the magnetic field to electrical energy at the output port of the piezoelectric material it is important to operate the piezoelectric material at the resonant frequency of the structure. Ideally for the application under consideration the mechanical resonance frequency should be based around a point between the minimum impedance frequency (series resonance frequency) and the maximum impedance frequency (parallel resonance frequency) of the piezoelectric material. From Figure 10 it can be noted that a piezoelectric material of height h = 7 mm - 8 mm is required for the construction of the piezoelectric component if a mechanical resonance frequency of 130 kHz is to be achieved. The bulk compliance of PZT, s_{44} (under constant electric field) used was 30×10^{-12} m^2N^{-1} [10,11] while the relative permittivity was considered to be 200.

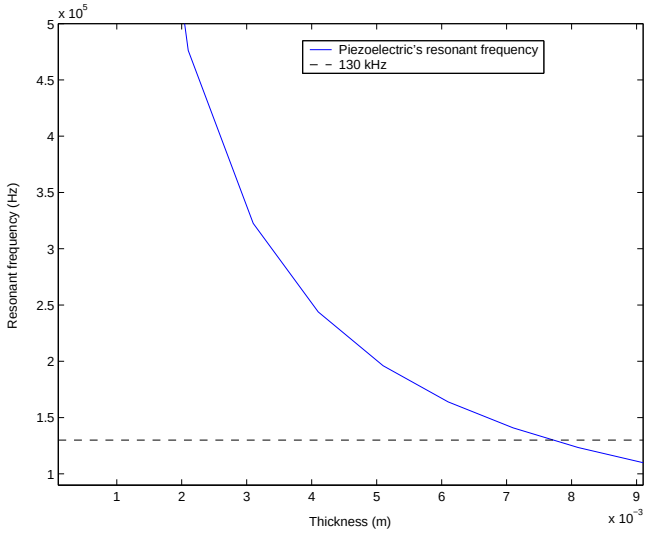

Figure 10: Resonant frequency of a PZT ceramic as a function of its thickness.

The magnetic material considered for the bar magnet should suitably have a high residual magnetisation M while occupying the largest possible volume. The latter is illustrated by both equations 20 and 27. Using a range of PtCo (Platinum and Cobalt) based alloys a residual magnetization M of 400,000 Am^{-1} is achievable. The bulk compliance of PtCo used in the evaluations was 10×10^{-12} m^2N^{-1}.

Figure 11 gives the variation in V_{EPR} at a distance of ½ meter from the loop structure generating the magnetic field. Here the effect of the width and the thickness of the piezoelectric are investigated, however the hight of the piezoelectric was fixed to ensure mechanical resonance.

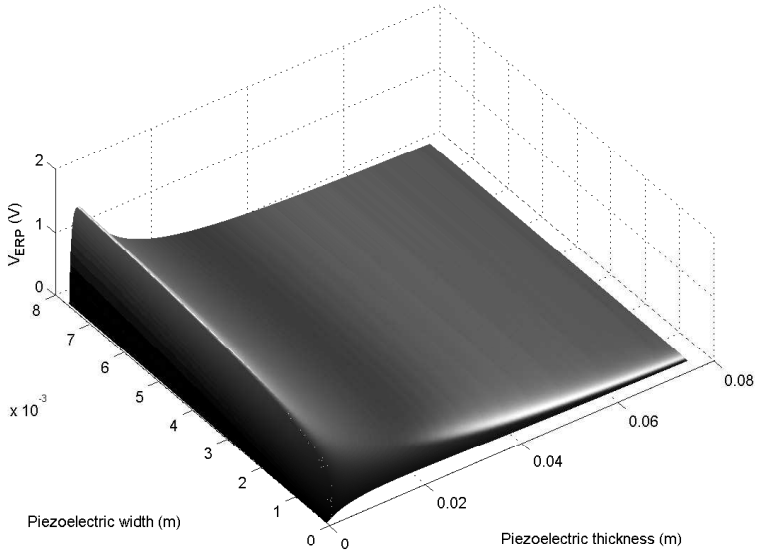

Figure 11: Effect of the piezoelectric structure dimensions on V_{EPR} at z = ½ meter from the "screaming corridor".

As can be seen from Figure 11, increasing the piezoelectric material has a gradually increasing effect on the energy that can be extracted from the electrical port. The width of the piezoelectric has a significant effect beyond 3 mm. It can be seen that V_{TO} is also a function of the thickness of the material. However there is an optimum value for the thickness of the piezoelectric to be used for a given width of the material.

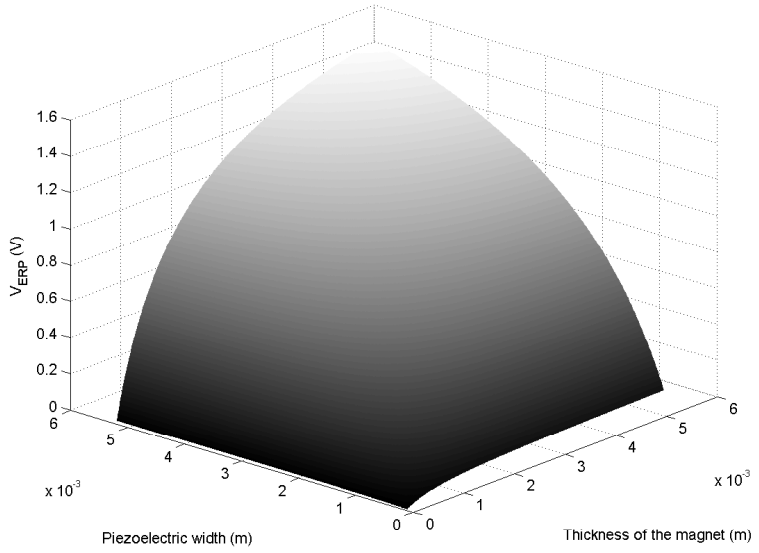

Figure 12: Effect of the magnetic structure dimensions on V_{EPR} at z = ½ meter from the "screaming corridor".

Figure 12, investigates the electrical power as functions of the width and thickness of the magnetic structure used in the application. As can be seen, V_{TO} is a strong function of the width of the magnetic structure as well as the thickness. This is as a result of the increase in the torque produced on the piezoelectric material by an increasing quantity of magnetic moment.

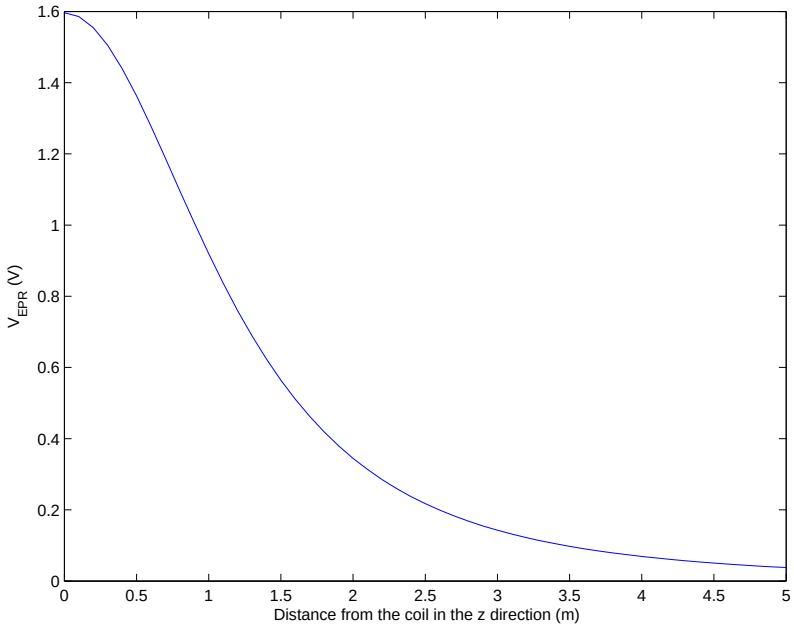

Figure 13: Turn-on range of the theft detection tag (measured from a "screaming corridor").

Based on the previous analysis, Figure 13 shows the V_{EPR} (V_{TO}) generated along a possible "screaming corridor". From the graph in Figure 13 a minimum operational distance of approximately 1 meter can be obtained for using the MEMS structure under consideration with the dimensions, w = 5 mm, t_p = 2 mm , t_m = 2 mm, and h = 7.5 mm considering the optimal dimensions to obtain an operating range of around 1 meter from the centre of the coil.

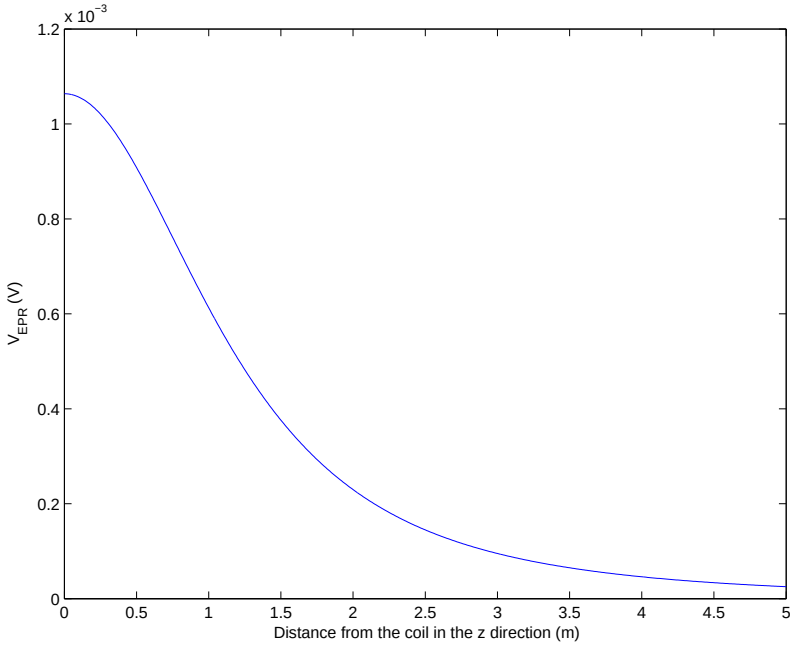

Figure 14: Turn-on range of the theft detection tag (measured from a "screaming corridor").

The mechanical *Q* of a piezoelectric material is very high, hence the MEMS device has a very narrow band resonance of around 100 Hz. Therefore it is important to note that as the frequency of the magnetic field is reduced below the mechanical resonant frequency the electrical impedance of the piezoelectric material increases. As a result it will greatly reduce the power transfer ratios while denying the benefit of a magnification of the energy at the electrical port. Figure 14 indicates the expected voltage from the device if mechanical resonance did not occur. In conjunction with the fact that the operating frequency is 130 kHz, the latter reality prevents other stray vibrations and fields from generating enough voltage to turn-on the theft detection circuits of the label and raising a false alarm. This emphasises the need to operate close to the resonance frequency of the piezoelectric material and the need to operate at a high enough frequency. However this may not always be practicable as it will depend largely on selecting suitable magnetic and piezoelectric materials with desirable characteristics to optimize the energy at the electrical port. In addition the cost of the structure will eventually determine a practical implementation in an active theft detection label.

5. CONCLUSIONS

There is an increasing demand for high performance anti-theft RFID labels. The development of active RFID labels has helped overcome performance barriers of passive labels and provided useful solutions to preventing theft of high value products. We have examined the problem of designing a theft detection circuit that does not drain the limited power supply of an active label but instead works to prolong the lifetime of the battery powered label while at the same time providing security implemented through a "screaming corridor". The MEMS device developed exploits a combination of magnetic and piezoelectric effects for the generation of a turn on voltages to a theft detection circuitry. We have used coupling relationships to investigate extraction of mechanical energy from a magnetic field and investigated the feasibility of operating a trigger system based on a combination of magetomechanical and piezoelectric effects within acceptable material volumes in a practical exciting field. The conclusion that sufficient energy transfer is possible has been established. We have also addressed the issue of adjusting material proportions to achieve resonance in the desired LF frequency range (100-135 kHz).

Future work will involve the investigation of the use of flexural mode to generate turn-on voltages and the study of the interplay between the electrode capacitance and the piezoelectric capacitance. The present size of the MEMS device needs to be further optimized to as to size and shape. Future work will also involve the simulation of the mechanical structure to confirm the results obtained from analytical methods.

REFERENCES

1. P. H. Cole, D. M. Hall, M. Loukine, and C. D. Werner, "Fundamental constraints on RF tagging systems", in *Proceedings of the fourth annual wireless symposium and exhibition*, Santa Clara, pp. 294-303, February 1995.
2. K. Eshraghian, P. H. Cole, and A. K. Roy, "Electromagnetic coupling in subharmonic transponders", in *Journal of Electrical and Electronic Engineering*, vol. 2, pp. 28-35,1982.
3. Hall, D. M. and Cole, P.H. "A fully integrable turn-on circuit for RFID transponders," in *Wireless and Portable Design Conference*, Burlington, Massachusetts, September 1997, pp 66-71.
4. Hall D, D. C. Ranasinghe and P. H. Cole "Turn on circuits based on standard CMOS technology for active RFID labels", submitted to *SPIE Conference on Microtechnologies for the new millennium*, Spain, 2005.
5. FCC website, http://www.fcc.gov.
6. C. B. William, and R. B. Yates, "Analysis of a micro-electric generator for Microsystems", in *Transducers '95/Eurosensors IX*, pp.369-372, 1995.
7. P. Glynne-Jones, S. P. Beeby, and N. M. White, "Towards a piezoelectric vibration-powered microgenerator", in *IEE Proceedings of Science, Measurement and Technology*,vol. 148, no. 2, pp.68-72, 2001.
8. Cole, P. H. "Coupling and Quality Factors in RFID", in *Design, Characterisation and Packaging for MEMS and Microelectronics*, Paul D. Franzon, Editor, Proceedings of SPIE Vol. 4593, pp 1-11, (2001).
9. B. A. Auld, *Acoustic Fields and Waves in Solids, Vol I*, John Wiley and Sons, pp. 265, New York, 1973.
10. Sensor technology limited webpage, http://www.morganelectroceramics.com/proptables.pdf, March 2005.
11. Advanced piezoelectrics, webpage http://www.piezotechnologies.com/k85.htm, March 2005.